Spin-polarised band structure for the semimagnetic semiconductor $Zn_{0.5}Mn_{0.5}Se$

1989 J. Phys.: Condens. Matter 1 5371

(http://iopscience.iop.org/0953-8984/1/32/006)

J. Phys.: Condens. Matter 1 (1989) 5371–5380. Printed in the UK

Spin-polarised band structure for the semimagnetic semiconductor $Zn_{0.5}Mn_{0.5}Se$

He Xiaoguang† and Huang Meichun‡

† Department of Physics, Xiamen University, Xiamen, People's Republic of China

‡ Centre of Theoretical Physics, CCAST (World Laboratory), Beijing and Department of Physics, Xiamen University, Xiamen, People's Republic of China

Received 27 May 1988, in final form 28 September 1988

Abstract. The spin-polarised band structure, density of states (DOS), magnetic moments and exchange interaction coefficients for a layer structure $Zn_{0.5}Mn_{0.5}Se$ in the ferromagnetic phase have been calculated using the self-consistent linear muffin-tin orbital atomic sphere approximation method. Its band structure and DOS distribution are explained through a p–d repulsion model. The band structure in the antiferromagnetic phase is also analysed qualitatively in terms of the p–d repulsion mechanism. The results of the present work show that the bands are strongly polarised. In the case of spin up, the bands are direct, with a band gap of 0.68 eV and a filled Mn 3d valence band whereas, for the spin-down case, the bands are indirect, with a band gap of 1.81 eV and an empty Mn 3d conduction band. These results are in agreement with Hund's rule. The calculated total magnetic moment is 4.81 μ_B/cell; the p–d and s–d exchange interaction coefficients are −1.10 eV and 0.04 eV, respectively.

1. Introduction

It is well known that $Zn_{1-x}Mn_xSe$ is a semimagnetic semiconductor (SMSC), in which a magnetic ion Mn^{2+} occupies the cation position in a II–VI semiconductor. The ion Mn^{2+} has a localised magnetic moment due to its half-filled 3d subshells. The interaction between the localised magnetic moment and valence electrons, in general, will lead to effective Landé factor g_{eff}, which depends strongly on the external magnetic field and the temperature. This causes much of the interesting magnetic and semiconducting behaviour, e.g. the extremely large Faraday rotation in the wide-gap SMSC, the low absorption coefficient and the strong magnetic field dependence of g_{eff} which are promising for optical non-reciprocal devices (e.g. isolators and modulators) and tunable Raman spin-flip lasers. On the contrary, because it is possible to control the dilution of the magnetic ion Mn^{2+} and because we have a good knowledge of the band structure of the II–VI host semiconductor, SMSCs are excellent materials for studying semiconductor and magnetic properties. For the above reasons, SMSCs have been widely investigated from both the experimental and the theoretical viewpoint during the past few years (Furdyna 1982, Galazka and Kossut 1980).

So far, in the SMSC family, $Cd_{1-x}Mn_xTe$ has been one of the materials most extensively studied. The spin-polarised band calculations for $Cd_{1-x}Mn_xTe$ have been performed by Larson *et al* (1985) using the augmented spherical-wave (ASW) method, Hass *et al* (1986) using the empirical tight-binding (ETB) method and Wei and Zunger (1987) using a

0953-8984/89/325371 + 10 $02.50

linear augmented plane-wave (LAPW) method. The relativistic effect has been partially considered in the LAPW calculation by Wei and Zunger, which leads to overlap between the Mn 4s bands and Mn 3d bands. The band structure exhibits a global similarity to ours. The magnetic parameters have been calculated within the Heisenberg model by Larson *et al*, but they did not give the results on the band structure and density of states (DOS) in detail. Although the band features of ASW calculation (Larson *et al* 1985) on MnTe are similar to those of the LAPW method (Wei and Zunger 1987), the important difference is that the Mn 4s bands do not overlap the Mn 3d bands, because the relativistic effects were neglected.

In this paper, we shall present some results of a theoretical investigation of the spin-polarised electronic structure for a new SMSC, $Zn_{0.5}Mn_{0.5}Se$, in the ferromagnetic phase. The calculated band structure and DOS can be discussed through a p–d repulsion model. We shall attempt to explain the photoluminescence (PL) peak under the band-edge peak in this system observed by the method of Bylsma *et al* (1986). The possibility of the p–d transition for this PL peak can be estimated using our calculated band parameters within the canonical band theory (Skriver 1984). The band for this compound in the antiferromagnetic phase is also qualitatively discussed on the basis of the band features in the ferromagnetic phase. Finally, the magnetic parameters obtained from our band calculation are given.

2. Method of calculation

The $Zn_{1-x}Mn_xSe$ system has a zincblende structure for the range $0 \leqslant x \leqslant 0.33$ and a wurtzite structure for $0.33 < x \leqslant 0.57$. It exists as a complex phase for $x > 0.57$. The magnetic phase diagram for $Zn_{1-x}Mn_xSe$ has been studied by Yang (1984).

Our first-principles calculation of the spin-polarised band for $Zn_{0.5}Mn_{0.5}Se$ was performed by the scalar relativistic linear muffin-tin orbital (LMTO) atomic sphere approximation (ASA) (Andersen 1975) within the local-spin-density functional approximation (LSDA) (von Barth and Hedin 1972). In this investigation, the von Barth–Hedin spin-polarised exchange correlation potential is used (von Barth and Hedin 1972).

For simplicity of calculation, we consider $Zn_{0.5}Mn_{0.5}Se$ to be an ideal wurtzite structure with lattice parameter $a = 4.083$ Å (Yorder-Short *et al* 1985) and $c = (8/3)^{1/2}a$. The unit cell is shown in the inset of figure 1, which can be seen as an alternating single-layer ZnSe/MnSe superlattice. In the self-consistency cycle, all core electrons are treated relativistically, while the valence electrons are treated semi-relativistically (Koelling and Harmon 1977), i.e. the spin–orbit coupling effect is neglected. The valence electrons that we have used in this calculation are Mn 4s, 4p and 3d, Se 4s, 4p and 4d and Zn 4s, 4p and 3d. The formula of the unit cell is $ZnMnSe_2$, i.e. it includes four atoms; thus we have a 36×36 secular equation. In order to save CPU time, in the first few iterations of our self-consistency cycle the band structure was evaluated at eight general $\boldsymbol{k}$-points inside the irreducible Brillouin zone. In the final few iterations, we increased the number of $\boldsymbol{k}$-points to 64. The solution is considered to be self-consistent when the difference between the total energy of two successive iterations differs by less than 4 mRyd. The resulting total and partial DOSs are shown in figures 2 and 3, respectively. To draw the band structure in figure 1, we made one final calculation of the energy eigenvalues in 81 $\boldsymbol{k}$-points with a regular distribution along the symmetry axis based on the self-consistent charge densities. All energies in the tables and figures are in electron volts and are referenced to the top of the spin-up valence band.

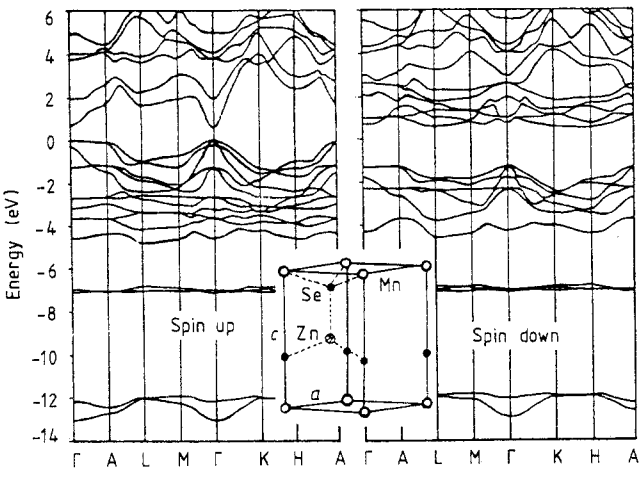

Figure 1. Structure model and spin-polarised band structure for $Zn_{0.5}Mn_{0.5}Se$.

3. Results and discussion

3.1. Band structure and density of states

The layer wurtzite structure $Zn_{0.5}Mn_{0.5}Se$ or $ZnMnSe_2$ can be seen as an ideal wurtzite $(ZnSe)_2$ in which half of the sites of the atom Zn are regularly substituted by the magnetic ions Mn^{2+}. In order to examine the changes in the band structure due to this atomic substitution, we have calculated the LMTO ASA band structure for the wurtzite ZnSe (He 1988). The results can be summarised as follows.

In the spin-up bands of $Zn_{0.5}Mn_{0.5}Se$, the electronic structure near the band edge is similar to that of wurtzite ZnSe. $Zn_{0.5}Mn_{0.5}Se$ has a direct gap with the extrema at the Γ point in the Brillouin zone. The most important differences between these two cases are as follows.

(i) The characteristic of the valence band of the SMSC is determined mainly by both the 3d orbitals on the Mn atoms and the 4p states on Se. The Mn 3d bands (spin-up) are almost completely mixed with the bands of Se 4p, because of a strong hybridisation with each other. Therefore the upper valence bands are constituted from five Mn 3d orbitals and six Se 4p, whereas the upper valence band of ZnSe consists of only Se 4p. At the same time, the dispersion of valence bands of the SMSC is less than that of ZnSe.

(ii) The degeneracy of the valence bands on some of the symmetry axis and high-symmetry points in Brillouin zone for the SMSC has been removed, because the group symmetry is lower than that of the wurtzite ZnSe.

For the spin-down case, the upper valence band in the SMSC system is constituted only from Se 4p orbitals, which is similar to that in ZnSe, but the degeneracy is lower, and the band width (six-band complex) is smaller than those of the spin-up case (11-band complex). The distinct differences between the spin-up and the spin-down band structure are as follows.

(i) The position of the 3d bands derived from the Mn atom is different. The Mn 3d bands for the spin-down case are emptied and are a primary part of conduction band; this can be seen from the distribution of the calculated partial DOS (figure 3).

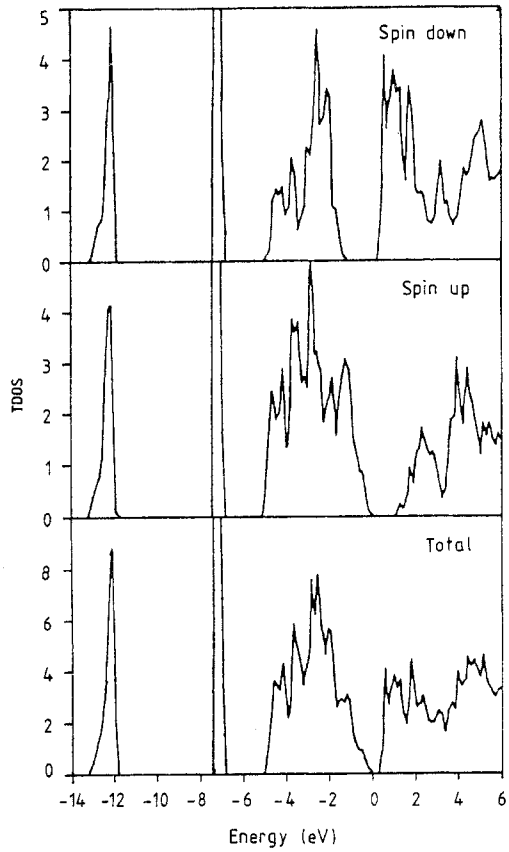

Figure 2. Total DOS.

(ii) The band-gap structure for the spin-down case is indirect with the conduction band bottom (CBB) at the P point (along the axes K–H and near the H point). This is because the p–d repulsion mechanism leading to the CBB at the Γ point causes the valence band maximum (VBM) to turn away at the Γ point. This picture therefore predicts a smaller spin-up direct band gap (0.68 eV) than the spin-down indirect band gap (1.81 eV).

On the whole, figures 1–3 and table 1 suggest that the VBM of spin-up bands is mainly formed by the hybridisation of Se 4p orbitals with Mn 3d orbitals, and the CBB by Zn 4s, Mn 4s and Se 4s. On the contrary, the VBM of spin-down bands is formed by Se 4p, the CBB (at P) is constituted primarily from Mn 3d with some Zn 3d character, and the CBB (at Γ) by Zn 4s with minor Mn 3d and Se 4s character.

In addition, our calculation suggests that the d–d exchange splitting Δ(d–d) (the energy separation of the d band centre between spin down and spin up) is 3.9 eV, and the p–d exchange splitting Δ(p–d) which can be expressed by the separation of the top of the valence bands for spin down and spin up, i.e. VBM(↓) − VBM(↑), is −1.25 eV. We have an effective negative p–d exchange splitting. This phenomenon shows that the effective potential for minority spin is more attractive than that for the majority spin, which is similar to the cubic system of the SMSC alloy $CdMnTe_2$ (Wei and Zunger 1987). The centre of the Mn 3d bands for spin up is located at −2.5 eV, which is higher than that (−2.9 eV) given by Webb *et al* (1981).

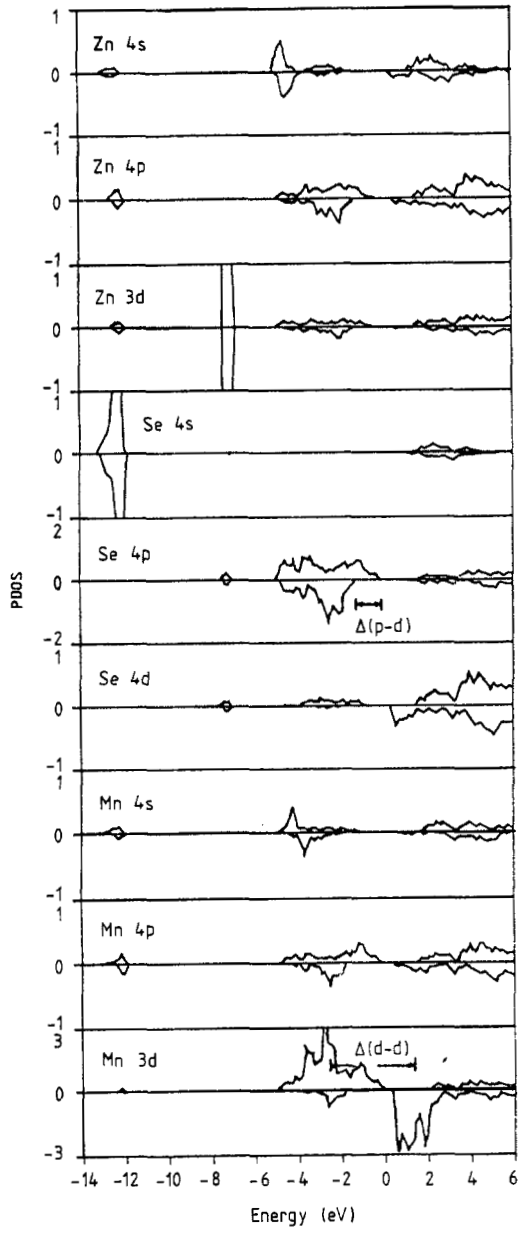

Figure 3. Partial DOS.

The band structure and partial DOS distribution described above can be explained in terms of the p–d repulsion mechanism. For this purpose, we consider that in fact the nearest atoms around the Mn atom have a regular tetrahedron symmetry (point group T_d); the representation for Mn 3d orbitals will be deduced to be a threefold degenerate Γ_{15} and a two fold degenerate Γ_{12} irreducible representation in the crystal field. In other words, the Mn 3d bands split into a triplet t_2 level and a doublet e level. For simplicity, let us assume that the influences of Mn and Zn on Se atoms are nearly the same; the crystal field for Se, therefore, can be considered to be of T_d symmetry. The corresponding

Table 1. Partial DOS (atoms and angular momenta percentages).

Spin-up states	Mn			Se			Zn			Spin-down states
	s	p	d	s	p	d	s	p	d	
				Near Γ point						
Γ_{3c}	0.5	16.7	0.7	0.0	6.8	46.9	0.3	27.0	1.0	
Γ_{2c}	29.3	3.1	9.2	22.8	5.0	20.3	2.9	4.0	3.4	
Γ_{1c}	7.2	1.3	5.7	31.5	11.4	3.7	35.0	2.5	1.9	
Γ_{1v}	0.0	8.8	43.4	0.0	44.2	0.9	0.0	0.2	2.6	
Γ_{2v}	3.3	7.8	41.8	4.6	37.3	0.9	2.6	0.1	1.8	
Γ_{3v}	0.9	5.6	32.0	0.1	48.7	1.9	0.3	2.8	7.6	
	0.2	0.9	80.3	1.0	1.8	11.7	1.4	1.5	1.3	Γ_{3c}
	0.2	1.0	79.3	1.3	2.0	11.7	1.5	1.6	1.3	Γ_{2c}
	5.4	2.1	13.4	27.2	8.8	6.7	32.5	1.0	3.0	Γ_{1c}
	0.0	0.4	5.1	0.0	69.8	0.8	0.0	12.0	11.9	Γ_{1v}
	0.2	0.7	4.5	2.0	65.4	1.3	3.7	10.7	11.7	Γ_{2v}
	0.0	1.3	25.7	0.5	60.2	2.3	0.4	3.9	5.8	Γ_{3v}
				At CBB (at P)						
	0.0	0.6	69.3	0.3	1.1	18.4	7.3	2.8	0.2	Γ_{2c}
	0.0	0.4	80.8	0.0	0.2	17.7	0.0	0.8	0.0	Γ_{1c}
	0.0	2.5	6.1	0.0	69.2	1.0	0.4	16.8	3.9	Γ_{1v}

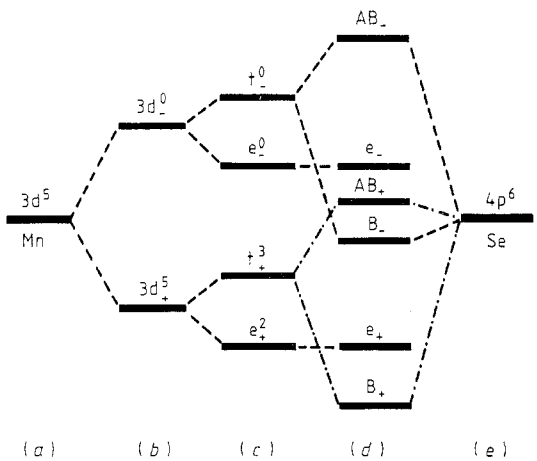

Figure 4. p–d repulsion scheme: (*a*) non-polarised d level; (*b*) polarised d levels; (*c*) splitting levels in the crystal field; (*d*) hybridised levels; (*e*) non-polarised p level in the covalent case.

representation for Se 4p in this field will be deduced to be a Γ_{15} irreducible representation. We know that the atomic level for Mn 3d is near that for Se 4p. As a result, the Se 4p will hybridise with the Mn 3d orbitals in the Γ_{15} channel, which produces a bonding state B and an anti-bonding state AB. Since the Mn 3d e states have a different transformation from the Se 4p states, there is no hybridisation in this channel. In the T_d symmetry environment, the e level is lower than the t_2 level. After hybridisation, the energy for the B state is lower than that for the AB state. Hence, we have the energy structure diagram shown in figure 4, where + and − denote spin up and spin down, respectively.

3.2. Antiferromagnetic band structure

The experimental study by Yang (1984) indicates that $Zn_{0.5}Mn_{0.5}Se$ is in the spin-glass phase. This means that an antiferromagnetic interaction exists between some of the Mn^{2+} ions. For this reason, it is necessary to discuss the band characteristic of antiferromagnetic $Zn_{0.5}Mn_{0.5}Se$. Unfortunately, this calculation is more complicated. Nevertheless, we can discuss the general features of the antiferromagnetic band structure on the basis of our results of ferromagnetic phase bands.

For the antiferromagnetic phase, the number of electrons for spin up should be equal to that for spin down because of the symmetry of the spin-polarised direction. Hence the antiferromagnetic $Zn_{0.5}Mn_{0.5}Se$ band structure can be imagined to be a whole energy level system made up of spin-up and spin-down bands. However, it is not a simple superposition of different spin bands, since now the Se 4p orbitals hybridise with the Mn 3d orbitals for both the valence and conduction band instead of with that for only the valence band. In this situation, the Mn 3d bands in the conduction band repulse the Se 4p bands, causing the VBM to turn down; at the same time, the Mn 3d bands in the valence band repulse the Zn 4s bands, leading the CBB to turn up. As a result, the energy gap becomes larger than that of a simple superposition of spin-up and spin-down bands. One can therefore predict that the dispersion of the valence and conduction bands, the absorption coefficient and the mobility will be smaller and the effective mass will tend to be larger. Because the spin-down bands in the ferromagnetic phase are indirect and the CBB (at Γ), of mainly s character, becomes higher, the antiferromagnetic band structure may be indirect.

Bylsma *et al* (1986) have performed PL and reflectivity measurements for $Zn_{1-x}Mn_xSe$. The results indicated that $Zn_{0.5}Mn_{0.5}Se$ is in the spin-glass phase with an energy gap of 3.1 eV and a PL peak under the band-edge peak (the so-called under-edge peak). On increasing the Mn^{2+} concentration ($x \geqslant 0.4$), the under-edge peak becomes more intense, while the band-edge peak becomes less intense and its full width at half-maximum becomes broader. They believed that the under-edge peak did not appear to be related to the transition from the valence band to conduction band, because the thermal shift of this peak (± 10 meV) is smaller than that of the band-edge peak (40 meV). They are also convinced that this peak cannot be due to Mn^{2+}-related intra-ionic transitions which occur at a much lower energy (2.1 eV or less) than their observation (about 3.0 eV).

According to our band calculation, we considered that the under-edge peak observed by Bylsma *et al* (1986) may be an indirect transition between CBB (at P) and VBM (at Γ), and the band-edge peak is derived from a direct transition between the CBB (at Γ) and VBM (at Γ). In general, the influence of the temperature on the band structure is often taken into account in terms of the effect of the temperature on the lattice constants. As already mentioned, the CBB (at P) mainly consists of Mn 3d, which participates less in the bonding with Se 4p than does Zn 4s. So the CBB (at P) is less influenced by temperature than is the CBB (at Γ). As a result, the thermal shift of the indirect transition (the under-edge peak) is qualitatively less than that of the direct transition (the band-edge peak).

The assignation for both PL peaks has been proved by our theoretical estimation. We have calculated the band centre C, the band width W and their volume variation (denoted by $dC/d(\ln S)$ and $dW/d(\ln S)$, respectively, where S is the atomic sphere radius) for both Mn 3d and Zn 4s conduction bands in the spin-down case using the Andersen's (1975) canonical band theory (He and Huang 1989). The results are listed in table 2. One can see that the band centre variation with respect to the crystal volume for Zn 4s

Table 2. ln S derivation of the centre of the band and the width.

Spin down	$dC/d(\ln S)$	$dW/d(\ln S)$
Mn 3d	−0.025	4.211
Zn 4s	0.329	2.822

Table 3. Magnetic moment calculated by us for $Zn_{0.5}Mn_{0.5}Se$.

Atom	Magnetic moment (μ_B/cell)
Mn	4.55
Se	0.18
Zn	0.08
$Zn_{0.5}Mn_{0.5}Se$	$\mu_{tot} = 4.81$

Table 4. Magnetic moments from Spalek (1986) for some SMSCs.

SMSC	Magnetic moment (μ_B/Mn)
$Cd_{1-x}Mn_xSe$	5.28
$Cd_{1-x}Mn_xTe$	4.94
$Hg_{1-x}Mn_xSe$	4.92

bands is much larger than for Mn 3d bands, whereas the variations in the band width for both Mn 3d and Zn 4s bands are of the same order of magnitude. These facts suggest that the temperature dependence of Zn 4s bands will be much more sensitive than that of the Mn 3d bands (CBB (at P)).

Perhaps it can also be interpreted in terms of chemical bonding. The interaction between Zn and Se produces a covalent-like bond, which is sensitive to temperature (or lattice parameter), whereas the Mn 3d states are relatively localised and independent of temperature (lattice parameter).

3.3. Magnetic parameters

In SMSCs, many of the interesting properties arise from the exchange interactions between the magnetic ions and the electrons near the band edges. In our problems, the local magnetic moments of the magnetic ion Mn^{2+} are determined by the spin angular momentum S, because the orbital angular momenta of the ions were quenched. If Mn 3d is completely polarised as in free space, its magnetic moment will be $gS\mu_B = 5.0\mu_B$ (where μ_B denotes the Bohr magneton). Our calculation for $Zn_{0.5}Mn_{0.5}Se$ yields a local magnetic moment for Mn of $4.55\mu_B$, small local magnetic moments for component atoms Se and Zn and a total magnetic moment of about $4.81\mu_B$/cell. The results are given in table 3. For comparison, the experimental magnetic moment data for some SMSCs (Spalek *et al* 1986) are listed in table 4. These data (in particular, the fact that the local

Table 5. Experimental data and our results on exchange coefficients.

	Calculated value (eV)		Experimental data (eV) (see text)	
N_α	0.04	0.29	0.24	0.26
N_β	−1.10	−1.40	−1.22	−1.31

magnetic moment of Mn is reduced to about $4.55\mu_B$) indicate that the Mn 3d electrons have an itinerant character due to the p–d hybridisation.

The other important magnetic parameters are the spin–spin exchange interaction constants N_α and N_β between the localised magnetic moment of the Mn 3d electrons and the band electrons. These two exchange constants can also be estimated from our ferromagnetic band structure. On the assumption that the exchange interactions between the Zn 4s conduction band electrons and Mn 3d electrons and between the Se 4p valence band electrons and Mn 3d electrons are the usual Kondo interactions, the exchange constants are defined as

$$N_\alpha = \Delta E_s / x\langle S_z\rangle$$

$$N_\beta = \Delta E_p / x\langle S_z\rangle$$

where $\langle S_z\rangle$ is the average Mn spin, and ΔE_s and ΔE_p are the band-edge spin splittings of the conduction band and valence band, respectively. From table 1, one can easily select the irreducible representations corresponding to the maximum Mn d, Se p and Zn s characters, for both spin up and spin down. Combining this information with our calculated eigenvalues, we found that $\Delta E_s = 0.0381$ eV and $\Delta E_p = -1.2498$ eV. Hence, we have calculated N_α and N_β using the $\langle S_z\rangle$ value for ferromagnetic $ZnMnSe_2$. The results and the experimental data (Heiman *et al* 1984, Twardowski *et al* 1983, 1984) for $x = 0.5$ are given in table 5. We can see that the exchange constant N_α is small and positive and N_β is large and negative and, qualitatively, the agreement is reasonable.

4. Conclusion

We have performed spin-polarised band-structure calculations for the SMSC $Zn_{0.5}Mn_{0.5}Se$ in the ferromagnetic phase. It was found that the most important difference between the spin-up and spin-down bands is the position of the 3d bands derived from the Mn atom. For the spin-up case, the Mn 3d bands are occupied, mixed with Se 4p bands and form the upper valence band with a direct band-gap structure whereas, in the spin-down case, the Mn 3d bands as a primary component of the conduction band are empty with an indirect band-gap structure. These results can be explained by a p–d repulsion mechanism. Our calculations and discussions on antiferromagnetic $Zn_{0.5}Mn_{0.5}Se$ show that the band centres for Mn 3d and Zn 4s are quite different from each other in their temperature dependences. This indicates that similar behaviours for these two CBBs will be valid in a rigid-band approximation. The transition between the relatively stable Mn 3d CBB and VBM is a possible mechanism for the under-edge PL peak observed by Bylsma *et al* (1986). The calculated magnetic parameters are in reasonable agreement with the experimental data.

Acknowledgments

We would like to thank associate professors Wang Renzhi and Shen Yaowen for helpful discussions. This work was carried out on a FACOM M-340S at the Computing Center of Xiamen University and was supported by the National Science Foundation of China.

References

Andersen O K 1975 *Phys. Rev.* B **12** 3060–83
Bylsma R B, Becker W M, Kossut J and Debska U 1986 *Phys. Rev.* B **33** 8207–15
Furdyna J K 1982 *J. Appl. Phys.* **53** 7637–43
Galazka R R and Kossut J 1980 *Springer Lecture Notes in Physics* vol 133 (Berlin: Springer) p 245
Hass K C, Larson B E, Ehrenreich H and Charlsson A E 1986 *J. Magn. Magn. Mater.* **54–7** 1283
He X G 1988 *Academic Degree Thesis* Xiamen University
He X G and Huang M C 1989 to be published
Heiman D, Shapira Y and Foner S 1984 *Solid State Commun.* **51** 603–6
Koelling D D and Harmon B N 1977 *J. Phys. C: Solid State Phys.* **10** 3107–14
Larson B E, Hass K C, Ehrenreich H and Charlsson A E 1985 *Solid State Commun.* **56** 347–50
Skriver H L 1984 *The LMTO Method* (Berlin: Springer) pp 17–111
Spalek J, Lewicki A, Tarnawski Z, Furdyna J K, Galazka R R and Obuszko Z 1986 *Phys. Rev.* B **33** 3407–18
Twardowski A, Dietl T and Demianiuk M 1983 *Solid State Commun.* **48** 845–8
Twardowski A, von Ortenberg M, Demianiuk M and Pauthenet R 1984 *Solid State Commun.* **51** 849–52
von Barth U and Hedin L 1972 *J. Phys. C: Solid State Phys.* **5** 1629–42
Webb C, Kaminska M, Lichtensteiger M and Lagowski J 1981 *Solid State Commun.* **40** 609–11
Wei S H and Zunger A 1987 *Phys. Rev.* B **35** 2340–65
Yang Y Q 1984 *Acta Phys. Sin.* **33** 1454–8 (in Chinese)
Yorder-Short D R, Debska U and Furdyna J K 1985 *J. Appl. Phys.* **58** 4056–60